PHYSICAL REVIEW B VOLUME 40, NUMBER 5 15 AUGUST 1989-I

Generalized norm-conserving pseudopotentials

D. R. Hamann
AT&T Bell Laboratories, 600 Mountain Avenue, Murray Hill, New Jersey 07974
(Received 16 March 1989)

A method is introduced for computing norm-conserving pseudopotentials from all-electron atom potentials at arbitrary energies, rather than at bound-state energies only, as in existing methods. This is shown to introduce considerable additional flexibility and convenience in constructing these potentials, and in dealing with certain "problem" atoms. As an example of such a case, pseudopotential and all-electron calculations of the electronic structure and structural energy of bulk BaSe are compared.

I. INTRODUCTION

Pseudopotentials simplify electronic-structure calculations by eliminating the need to include atomic core states and the strong potentials responsible for binding them. The widely used norm-conserving pseudopotentials (NCPP's) have several desirable properties.[1] They are calculated from *ab initio* self-consistent atomic potentials based on local-density-functional (LDF) theory. They produce nodeless valence wave functions which converge to become identical to normalized full-potential wave functions beyond a chosen "core radius" r_c, and are themselves properly normalized. This latter property is essential for producing a correct description of bonding in pseudopotential calculations, and correct self-consistent electrostatic and exchange-correlation potentials. Simultaneously, NCPP's reproduce the scattering power of the full atom potential correctly at energies away from the bound-valence-state energy to first order in the energy difference. When constructed according to a well-designed procedure, they in fact reproduce it over a much wider range than the rigorous "first-order" result would indicate.[1]

As a result, NCPP's reproduce all-electron electronic-structure calculations with a high degree of accuracy.[1] They have been calculated and tabulated for every atom in the Periodic Table.[2] They have been shown to give results in excellent agreement with experiment for lattice constants, elastic properties, vibrational frequencies, and structural phase transitions.[3] Despite the fact that the published NCPP's (Ref. 2) are derived for use in LDF calculations, they have recently been shown to accurately reproduce valence energies in Hartree-Fock and many-body-perturbation-theory calculations.[4]

Why tamper with something that works so well? There are several reasons. NCPP's are local functions of radius, but different functions for each angular momentum l. In a molecule or solid, wave functions contain all l components about each atom, and it is typically necessary to have NCPP's up to $l_{\max}=2$ or 3. (This potential is usually taken as the "local" potential which applies to all higher l's.) States with l's which are not among the occupied valence orbitals in the atomic ground configuration are at best weakly bound, and often unbound in the LDF atomic potential. As a result, it is necessary to use additional ionized configurations to obtain satisfactory NCPP's for these l's.[2] The desired functions for use in electronic-structure calculations are the bare-ion NCPP's, which are obtained from the atomic NCPP's by "unscreening," that is, by subtracting the electrostatic and exchange-correlation potentials of the pseudocharge density.[1,2] While the basic transferability of NCPP's ensures a high degree of consistency among bare-ion NCPP's derived from different configurations,[1] the use of multiple configurations is an inconvenience and a possible source of error. This possibility is greatest for alkali atoms, where configurations containing only a fraction of an electron must be used for $l=1$, 2, or 3,[2] and the nonlinearities of the exchange-correlation functional have the greatest opportunity to introduce unscreening inconsistencies.[5]

Another class of problems is posed by Cs and Ba. These atoms have a narrow resonance in the $l=3$ channel at positive energies. To obtain an $l=3$ NCPP, a bound f state must be created by using an ionized configuration, and it is highly localized. The resulting potential is extremely strong (~ -100 hartrees for Ba),[2] which makes the use of plane-wave expansions essentially impossible. For many applications, it would be perfectly adequate to permit errors around the energy of the f resonance if the f scattering of the atoms at lower energies could be represented properly by a weak potential. A third kind of problem concerns rare gases. For some applications, such as rare-gas–surface interactions, we may only be interested in their repulsive interactions with electrons near the Fermi level, and not in their deeply bound closed shells of valence electrons. Existing methods[1,2] based on bound states offer no way of deriving such NCPP's.

The generalized approach to NCPP's introduced here is based upon the recognition that calculations completely parallel to those using bound states can be introduced for arbitrary energies.[6] Atomic wave functions at arbitrary energies in the valence range which are regular at $r=0$ diverge as $r\to\infty$. They would seem to be poorly defined objects, especially in terms of normalization.

However, in a solid or molecule, such diverging wave functions are "captured" by the potentials of neighboring atoms. Stated in other terms, these wave functions represent the tails of valence orbitals centered on other atoms. The requirements that they be properly scattered by the atom being discussed, and that they have the right amount of charge in its vicinity, are in fact well defined in this context. The theory for calculating such potentials is discussed in Sec. II.

Car and Parrinello recently introduced methods for greatly increasing the computational efficiency of plane-wave pseudopotential calculations based upon treating the action of the potential-energy operator on wave functions in real space.[7] The kinetic energy operates in Fourier space, and the two representations are efficiently related by fast Fourier transforms. The l nonlocality of NCPP's makes the real-space operation essentially impossible. A separable approximation to the NCPP introduced by Kleinman and Bylander retains the norm-conserving property,[8] and can be used in the Car-Parrinello approach without sacrificing the efficiency of real-space operation.[9] Since the Kleinman-Bylander form uses the pseudo-wave-function multiplicatively, it would appear to be incompatible with the new generalized NCPP. We show in Sec. III, however, that under rather weak restrictions a parallel separable form is well defined.

In Sec. IV, we discuss sample results illustrating the use of generalized NCPP's (GNCPP's), concentrating on the rocksalt-structure compound BaSe. This example illustrates both the solution of the "f problem" for Ba, and the flexibility of GNCPP's in a situation where several levels may optionally be treated as core or valence electrons. Our observations are summarized in Sec. V. Finally, in the Appendix, we briefly describe the structure of a Fortran program for computing GNCPP's which the author will make available to interested readers.

II. CONSTRUCTION OF GNCPP's

The first step is to calculate the self-consistent LDF potential $V(r)$ for the atom of interest, typically using the ground configuration. For the results reported here, we used the scalar-relativistic version of the Schrödinger equation, which contains the mass-velocity and Darwin corrections, but is averaged over the spin-orbit term.[10] The equation satisfied by $u_l(r)$, which is r times the radial wave function, is

$$-\frac{d^2u_l}{dr^2}-\frac{\alpha^2}{2M}\frac{dV}{dr}\left[\frac{du_l}{dr}-\frac{u_l}{r}\right]+\left[\frac{l(l+1)}{r^2}+2M(V-\varepsilon)\right]u_l=0 \quad (1)$$

in hartree atomic units, where

$$M=1-\tfrac{1}{2}\alpha^2(V-\varepsilon)\ , \quad (2)$$

and α is the fine-structure constant. The relativistic corrections are only important in the inner core region. Following past practice, these will be incorporated into the final pseudopotential, so that a solution of the nonrelativistic Schrödinger equation using that potential will reproduce the relativistic effects along with other core-region effects in the scattering.[2,11,12]

For angular momenta l for which bound valence states occur, it makes sense to follow the existing prescription and derive the NCPP at the bound-state energy.[1] This is typically the energy at which valence or low-lying conduction bands will have that l as their dominant angular-momentum character. For other l, we simply pick an energy ε_l. The energy of the highest occupied valence state is an obvious choice.

The next step is to choose the "core radius" r_{cl}. We recall that for bound states, this is typically chosen to be 0.4 to 0.6 times the radius at which $u_l(r)$ has its outermost maximum.[1,2] This will force the pseudo-wave-function to converge to the full-potential wave function somewhat inside this maximum, which typically occurs near the relevant radius for bonding. For the generalized case, the wave function is typically diverging with increasing r, and a different criterion is needed. If there is a bound core state for l, r_{cl} must be large enough that the pseudo-wave-function converges to the full-potential wave function outside the outermost maximum of the highest lying such core state. Taking r_{cl} to be 2 to 3 times the radius of that maximum is a rule which, when applied to bound states, gives values which are similar to those found from the usual guidelines. This provides a lower bound for r_{cl} for the unbound states. If this value is smaller than the largest r_{cl} among the l's for the bound states of the atom, we can use this larger value. Convergence of the full-potential wave functions and pseudo-wave-functions for l's without a bound state at radii smaller than those of the valence states tends to make the pseudopotentials stronger, and serves no purpose. We also must choose a functional form to enforce our r_{cl} cutoffs, and the choice

$$f(r/r_{cl})=\exp[-(r/r_{cl})^{\lambda}]\ , \quad (3)$$

with $\lambda=3.5$, has proven effective.[2] These choices now enable us to pick an outer radius at which the pseudo-wave-function can be accurately converged to the full-potential wave function, $R_l\sim 2.5r_{cl}$. We then integrate Eq. (1) with $\varepsilon=\varepsilon_l$ outward from the origin, starting with an appropriate power series for u_l which goes to zero at the origin. We stop the integration at R_l, and normalize u_l so that

$$4\pi\int_0^{R_l}u_l^2\,dr=1\ . \quad (4)$$

We save the normalized value $u_l(R_l)$ and first derivative $u_l'(R_l)$. Choosing R_l significantly larger than needed causes the outermost part of the diverging wave function to completely dominate the normalization integral, resulting in a serious loss of numerical accuracy in a subsequent part of the calculation. Another problem can occur with large R_l for positive values of ε_l. In this case, the wave function will oscillate at large r, and if a node occurs between r_{cl} and R_l, a later step in the GNCPP construction (inverting Schrödinger's equation) will fail. The joint requirements that r_{cl} be greater than the radius

of the outermost node in the core region and that $R_l \gtrsim 2.5 r_{cl}$ effectively limit the maximum energy at which the GNCPP construction is possible.

Following the standard procedure, we introduce an intermediate pseudopotential

$$V_{1l}(r)=[1-f(r/r_{cl})]V(r)+c_l f(r/r_{cl}) , \tag{5}$$

which converges to the full potential $V(r)$ for $r>r_{cl}$. V_{1l} is now used in a nonrelativistic Schrödinger equation, which is started with a power series going to zero at the origin and integrated outward to R_{cl} to find the intermediate wave function $w_{1l}(r)$. For bound states, c_l was adjusted to make the energy eigenvalues of the full potential and pseudopotential agree. For the present generalized case, we adjust c_l so that

$$\left.\frac{w'_{1l}}{w_{1l}}\right|_{R_l} = \left.\frac{u'_{1l}}{u_{1l}}\right|_{R_l} . \tag{6}$$

The most stable way to perform this adjustment is to treat the problem defined by Eq. (6) as a bound-state eigenvalue problem. Typically, one solves bound-state problems by integrating the Schrödinger equation outward from the origin to a radius near the classical turning point at a trial energy, and inward from a large radius to this same point. The values are matched, the resulting function normalized, and the slope discontinuity used to improve the trial energy by first-order perturbation theory.[13] The same approach can be used substituting Eq. (6) for the result of the inward integration, and normalizing only inside R_l. For a trial value $c_l^{(n)}$ used in Eq. (5), this procedure yields an "eigenvalue" $\varepsilon_l^{(n)}$, and the perturbational correction

$$c_l^{(n+1)}=c_l^{(n)}+\frac{\varepsilon_l-\varepsilon_l^{(n)}}{\int_0^{R_l} f(r/r_l)[w_{1l}^{(n)}(r)]^2 dr} \tag{7}$$

iteratively converges to the desired c_l. The more direct procedure of keeping ε_l fixed for the outward integration and iteratively improving c_l to satisfy Eq. (6) has proven to be unstable.

From here on, the procedure is completely standard. A scale factor is found to make the full potential and pseudo-wave-functions identical at R_l,

$$\gamma_l = u_l(R_l)/w_{1l}(R_l) , \tag{8}$$

and the final pseudo-wave-function constructed by adding a short-ranged norm-correcting term,

$$w_{2l}(r)=\gamma_l[w_{1l}(r)+\delta_l g_l(r)] . \tag{9}$$

δ_l is the smaller solution of the quadratic equation resulting from the condition that w_{2l} be normalized,

$$\gamma_l^2 \int_0^{R_l} [w_{1l}(r)+\delta_l g_l(r)]^2 dr = 1 . \tag{10}$$

It it usually adequate to choose g_l to be

$$g_l(r)=r^{l+1} f(r/r_l) . \tag{11}$$

The final pseudopotential, found from analytically inverting the Schrödinger equation, is then[1,2]

$$V_{2l}(r)=V_{1l}(r)+\frac{\gamma_l \delta_l r^{l+1} f(r/r_{cl})}{2w_{2l}(r)}\left[\frac{\lambda^2}{r^2}\left[\frac{r}{r_{cl}}\right]^{2\lambda}-\frac{2\lambda l+\lambda(\lambda+1)}{r^2}\left[\frac{r}{r_{cl}}\right]^{\lambda}+2\varepsilon_l-2V_{1l}(r)\right] . \tag{12}$$

The key identity which ensures the transferability of norm-conserving pseudopotentials is[1,2,14]

$$-\frac{1}{2}\left[u_l^2 \frac{d}{d\varepsilon_l}\frac{d}{dr}\ln\frac{u_l}{r}\right]_R = \int_0^R u_l^2 dr . \tag{13}$$

For either u_l or w_{2l}, at $R=R_l$ the right-hand sides of Eq. (13) are the same by construction, as are $d\ln(u_l/r)/dr$ and $d\ln(w_{2l}/r)/dr$. This implies that the logarithmic derivatives at energy ε are the same to first order in $(\varepsilon-\varepsilon_l)$, so the scattering power of V_{2l} for l partial waves is the same as that of the full potential $V(r)$ to a good approximation at energies away from the selected energy.[1,2] Whether or not the energies and wave functions in Eq. (13) correspond to bound states plays no role in this transferability argument, and the identity is valid in either case. This observation motivated the present extension to the general case. There is every reason to believe that, for choices of r_{cl} which give reasonable-looking, smooth potentials, the transferability extends to energies considerably beyond the energy range suggested by Eq. (13), as found previously.[1] Of course, when ε_l is deliberately set to avoid a sharp resonance, the pseudopotential cannot be expected to reproduce that resonance.

In contrast to the case of bound-state-only pseudopotentials found for several different atomic configurations,[2] a single valence-electron electrostatic and exchange-correlation potential can be subtracted from all V_{2l} to find the full set of ionic pseudopotentials,

$$V_l^{\rm ion}(r)= V_{2l}(r)-\frac{4\pi}{r}\int_0^r \rho(r')r'^2 dr' -4\pi\int_r^\infty \rho(r')r'\,dr'-\frac{\delta E_{\rm exc}[\rho(r)]}{\delta\rho(r)} , \tag{14}$$

where

$$\rho(r)=\sum_l n_l[w_{2l}(r)/r]^2 . \tag{15}$$

In the above, n_l is the occupancy of bound valence state l. In the case of rare gases, when all the electrons in the ground configuration are being treated as core, there is no unscreening, and $V_l^{\rm ion}(r)=V_{2l}(r)$.

III. SEPARABLE GNCPP's

In applying GNCPP's, they must operate on basis functions which are not, in general, eigenfunctions of l about the ion. Because $V_l^{\rm ion}$ is l dependent, matrix elements of the ionic potential must be calculated as

$$\langle\phi_1|V^{\rm ion}|\phi_2\rangle=\sum_{l,m}\int d\mathbf{r}\int d\mathbf{r}'\,\phi_1^*(\mathbf{r})Y_{lm}(\hat{\mathbf{r}})V_l^{\rm ion}(r)\delta(r-r')Y_{lm}^*(\hat{\mathbf{r}}')\phi_2(\mathbf{r}')\ , \tag{16}$$

where the ion is assumed to be at the origin. As discussed in the introduction, this form is computationally inconvenient for some applications, and Kleinman and Bylander proposed a fully separable form which can have computational advantages.[8] With their form, the matrix element between general basis functions becomes

$$\langle\phi_1|V_{\rm KB}^{\rm ion}|\phi_2\rangle=\int d\mathbf{r}\,\phi_1^*(\mathbf{r})V_{\rm loc}^{\rm ion}(r)\phi_2(\mathbf{r})+\sum_{l,m}C_l\int d\mathbf{r}\,\phi_1^*(\mathbf{r})Y_{lm}(\hat{\mathbf{r}})Q_l^{\rm ion}(r)\int d\mathbf{r}'\,Y_{lm}^*(\hat{\mathbf{r}}')Q_l^{\rm ion}(r')\phi_2(\mathbf{r}')\ . \tag{17}$$

In the above, we have introduced the radial function

$$Q_l^{\rm ion}(r)=[V_l^{\rm ion}(r)-V_{\rm loc}^{\rm ion}(r)][w_{2l}(r)/r]\ , \tag{18}$$

and the coefficient

$$C_l=\left[4\pi\int_0^\infty Q_l^{\rm ion}(r)w_{2l}(r)r\,dr\right]^{-1}\ . \tag{19}$$

As introduced, $w_{2l}(r)$ were bound pseudo-wave-functions, and the choice of the "local" pseudopotential $V_{\rm loc}^{\rm ion}(r)$ was essentially arbitrary.[8] The exponential decay of the pseudo-wave-functions made the integrals in Eqs. (18) and (19) converge. Substituting Eq. (18) back into the atomic problem (and adding the screening potential from the occupied pseudo-wave-functions), it is easily seen that the Schrödinger equation for each l is satisfied by construction.[8] It may also be shown that Eq. (13), and hence first-order transferability in $(\varepsilon-\varepsilon_l)$, is preserved by the separable form.[15] Wide-energy-range tests of the logarithmic derivatives such as those given in Ref. 1 have not been reported for the Kleinman-Bylander separable form.

The immediately apparent problem in generalizing this separable form to arbitrary energies is the divergence of $w_{2l}(r)$ at large r. The other factor which can converge these integrals is $(V_l^{\rm ion}-V_{\rm loc}^{\rm ion})$. If this factor goes to zero faster than $(w_{2l})^2$ goes to infinity, the integrals will be finite. A simple and computationally expedient way to satisfy this requirement is

$$V_{\rm loc}^{\rm ion}(r)=V_{l_{\rm max}}(r)\ , \tag{20}$$

where $l_{\rm max}$ is the largest l for which a GNCPP is computed. Since all $V_l^{\rm ion}$ converge to the same potential for $r>r_{cl}$ as $f(r/r_{cl})$, and any practical f goes to zero much more rapidly than an exponential, convergence of the integrals is assured. With this choice, the lm sum in Eq. (19) terminates at $l_{\rm max}-1$. If one gives up this computational savings, any sufficiently short-ranged function could be added to the right side of Eq. (20). While Kleinman and Bylander suggested that adjusting $V_{\rm loc}^{\rm ion}$ could improve transferability of the separable potential,[8] they did not give any systematic way of doing so, and we have not explored this possibility further.

IV. APPLICATION TO SOLIDS

Initial tests were carried out comparing plane-wave-pseudopotential (PWPP) and linear-augmented-plane-wave (LAPW) calculations for Si. Since only the $l=2$ GNCPP differed from the bound-state form (typically found from a Si^{2+} configuration), no surprises were expected. In fact, the band structures, lattice constants, cohesive energies, and bulk moduli agreed among the three calculations (LAPW, PWPP, and PWPP separable) within essentially numerical accuracy.

For a test which would better illustrate the advantages of the GNCPP, we wanted to use a simple semiconducting compound containing Ba. As discussed in the introduction, Ba has a low-lying f resonance. This leads to an extremely localized bound f state for the Ba^+ configuration conventionally used for $l=3$ pseudopotential, which is hence extremely strong and short ranged.[2] Among several rocksalt-structure Ba chalcogenides we chose BaSe, because Se is the first chalcogen with a d core. We have no reason to believe that this compound has any particularly interesting physical properties. The highest occupied atomic levels (local-density eigenvalues, actually) are $5p$ and $6s$ at -18.7 and -3.5 eV for Ba, and $4s$ and $4p$ at -17.4 and -6.7 eV for Se. It is clear from these numbers that there are two ways to treat the compound: either the bands arising from all these levels should be included, or only those from the Ba $6s$ and Se $4p$ electrons should. This provides a further test of the flexibility of the GNCPP approach.

The wave functions entering into the generalized construction method are illustrated in Fig. 1 for Ba and

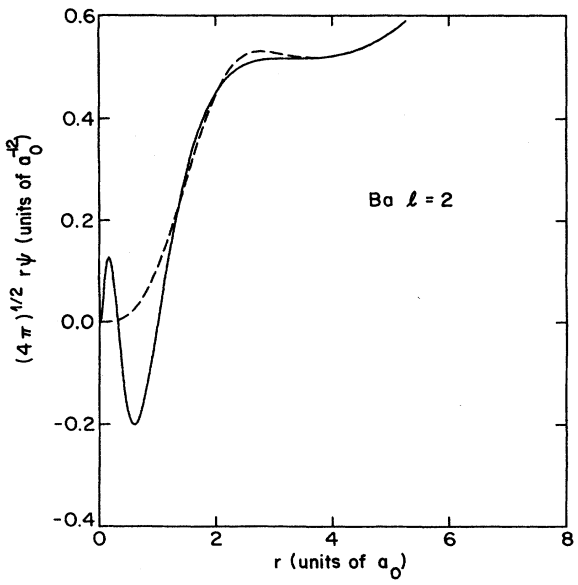

FIG. 1. Diverging Ba $l=2$ wave functions for the full potential (solid line) and pseudopotential (dashed line) at $\varepsilon_2=-0.128$ hartrees.

$l=2$. In this case, we chose $r_{c2}=2.2$ atomic units (a_0), leading to $R_2=5.26$ a.u. The manner in which the full-potential wave function (solid line) and pseudo-wave-function (dashed line) merge is qualitatively similar to their behavior for bound states (see Fig. 1 of Ref. 1 or Fig. 6 of Ref. 2). While a substantial fraction of the "normalization" integral of these wave functions is outside their "merge point," this choice of R_2 keeps that fraction from overwhelming the weight in the inner region.

Two possible choices of pseudopotentials for Ba and Se are shown in Figs. 2 and 3. Both are based on the ground configuration for the atoms. In Fig. 2, only the Ba $6s$ and Se $4p$ electrons are treated as valence, and the pseudo-ions are Ba^{2+} and Se^{4+}. The potential in Fig. 3 is based upon including the Ba $5p$ and Se $4s$ electrons in the valence shell as well, and we have Ba^{8+} and Se^{6+} pseudo-ions. The r_{cl} and ε_l used in these calculations are given in Table I. A comparison between the Se $l=2$ potential in Fig. 3 and one calculated using the bound-state method with an $s^1p^{2.75}d^{0.25}$ ionic valence configuration[2] shows that these potentials are very similar. It is clear that all the potentials are weak within the scale set by the ionic charge. They have no "kinks" or "wiggles," which is an important heuristic criterion for wide transferability.[1,2] We give a direct comparison between the Ba^{2+} $l=3$ potential from Fig. 2 and one calculated using the bound-state method with the configuration and r_{c3} from Ref. 2 ($s^{0.75}f^{0.25}$, 0.274 a.u.) in Fig. 4. The convergence difficulties in using the bound-state potential in a plane-wave expansion are readily apparent.

For reference, self-consistent linear-augmented-plane-wave calculations of the band structure and of the cohesive energy versus lattice parameter were carried out. These calculations are based on all-electron potentials, and make no shape approximations for the potential or charge density.[16] Bands arising from the As $4s$, As $4p$, Ba $5p$, and Ba $6s$ atomic levels were treated as valence bands, and deeper bands were treated in the rigid-core approximation. Muffin-tin radii are chosen as 3.39 a.u. for Ba, and 2.44 a.u. for Se. The interstitial wave func-

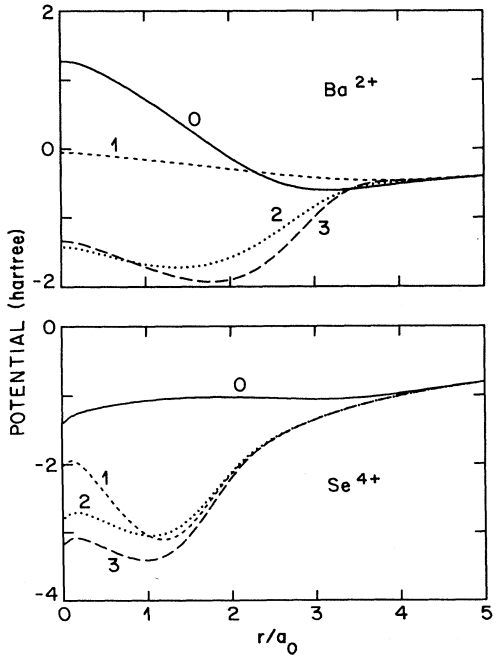

FIG. 2. Ba^{2+} and Se^{4+} ionic pseudopotentials. The curves are labeled by l.

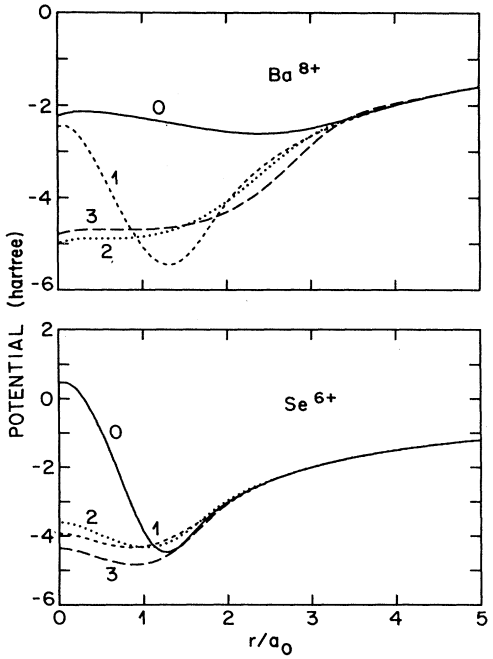

FIG. 3. Ba^{8+} and Se^{6+} ionic pseudopotentials. The curves are labeled by l.

TABLE I. Parameters for the pseudopotentials in Figs. 2 and 3.

Ion	l	ε_l (hartrees)	r_{cl}/a_0
Ba^{2+}	0	−0.138	2.41
	1	−0.128	3.17
	2	−0.128	2.41
	3	−0.128	2.41
Ba^{8+}	0	−0.128	2.41
	1	−0.687	1.20
	2	−0.128	2.20
	3	−0.128	2.41
Se^{4+}	0	−0.050	2.84
	1	−0.245	1.20
	2	−0.050	1.60
	3	−0.050	1.60
Se^{6+}	0	−0.640	1.05
	1	−0.245	1.40
	2	−0.245	1.45
	3	−0.245	1.50

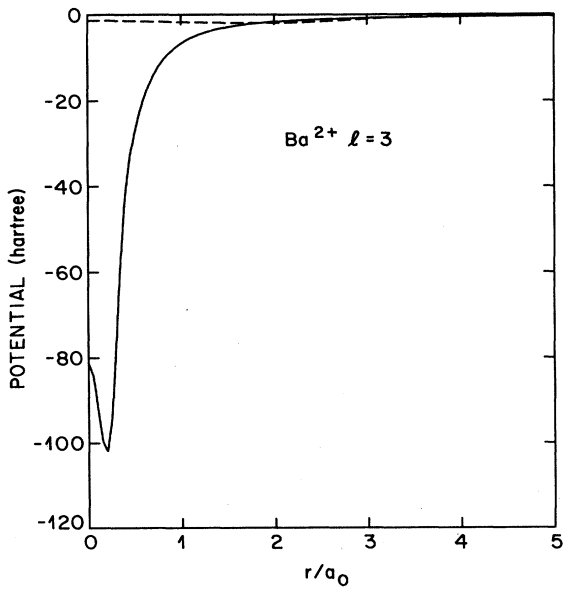

FIG. 4. Ba^{2+} $l=3$ pseudopotential from Fig. 2 (dashed line) and constructed from a bound f state (solid line) following Ref. 2.

tions and potentials are expanded in plane waves with kinetic energies up to 9 and 70 Ry, respectively. The muffin-tin wave functions and potentials are expanded in spherical harmonics up to $l=6$. A six-special-point Brillouin-zone sample is used.[17] Experience has indicated that these choices yield bands and cohesive energies converged to ~ 0.1 eV for such materials.

The LAPW band structure is shown in Fig. 5(a). The shallow core bands from -8.5 to -12.5 eV are hybrids of Ba $5p$ and Se $4s$. The Se $4p$ "valence" band lies between -2.2 and 0 eV. The conduction bands from 1.7 to 8.5 eV have predominantly Ba $6s$ and $5d$ character. The Ba $4f$ bands are clustered between 8.5 and 10 eV. We expect that the band gap is seriously underestimated compared with experiment as in typical local-density-functional calculations for semiconductors.

A pseudopotential band structure was calculated using the Ba^{2+},Se^{4+} potentials shown in Fig. 2 and a plane-wave basis set with a maximum kinetic energy of 10 Ry. This set of approximately 260 plane waves gave good convergence, and a band structure in excellent agreement with the LAPW result for the anticipated bands, as seen in Fig. 5(b). Differences are in the 0.1-eV range for the valence and low-lying conduction bands, and grow to a few tenths of an eV in the higher conduction bands. The shallow core bands and the Ba $4f$ conduction bands are, of course, absent.

Another calculation was performed using the Ba^{8+} and Se^{4+} potentials shown in Fig. 3. The shallow core bands are, of course, considerably harder to converge, and a basis of approximately 480 plane waves with maximum energy of 15 Ry was necessary to bring these bands to within ~ 0.3 eV of the LAPW reference results. This set of bands is shown in Fig. 5(c). The excellent quality of agreement in the Se valence and Ba conduction bands is maintained, and the Ba $4f$ bands remain absent as intended.

A band calculation using the separable forms of these same potentials was also carried out.[8] In contrast to our result with Si, the results were less than satisfactory. Errors in the range of 0.5–1 eV were found, both within and between groups of bands. We speculate that the states in the solid are sufficiently modified from the atom states used as projection operators that the transferability suffers. The errors were comparable for bands with symmetries related to both bound-state and generalized-state components of the pseudopotential. While it may have been possible to improve the bands by adjusting the local part of the potential to be something other than the $l=3$ component,[8] we know of no systematic way to do so. There is very little in the literature documenting the per-

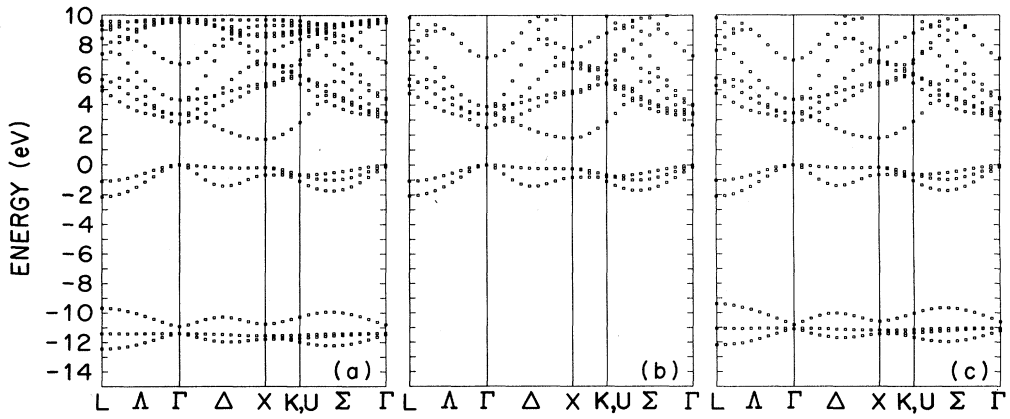

FIG. 5. Band structures for BaSe based on (a) full-potential LAPW calculations, (b) Fig. 2 pseudopotentials with plane-wave basis functions, and (c) Fig. 3 pseudopotentials with plane waves.

formance of the separable potentials, so it would be prudent to test them for each new situation before undertaking a major computational project.

A series of calculations of the total energy of BaSe as a function of lattice parameter was carried out to test the capabilities of the GNCPP's for structural predictions. The reference LAPW results are shown as the solid curve in Fig. 6. (All the cohesive energy curves are third-order polynomials least-squares fitted to seven calculated points.) The lattice parameter, the only experimental quantity available to us, is in very good agreement with experiment,[18] as seen in Table II. The "valence-only" GNCPP from Fig. 2 did not give satisfactory results. The dotted curve in Fig. 6 was calculated with this potential, and showed no sign of approaching a minimum within the range investigated. The shallow core bands clearly make an important contribution to interatomic repulsion. The GNCPP's incorporating these bands, however, give excellent structural results even when these bands are not well converged, as seen from the long-dashed curves in Fig. 6. The excellent quantitative agreement of the position and curvature of the minima is seen in Table II. Of course the cohesive energy is not converged at the 12.5-Ry cutoff used for the lower curve. The single cohesive energy calculated with a 15-Ry cutoff at the experimental lattice parameter is still 2 eV above the reference LAPW result. Despite its poor performance with the band energies, the separable version of the Fig. 3 potential gave respectable structural results, shown as the short-dashed curve in Fig. 6. The basis cutoff was 10 Ry for these calculations. The minimum lattice parameter is 1.3% smaller than the LAPW reference, as seen in Table II, but the bulk modulus is close to the other results. This level of performance would be suitable for many applications to structural problems.

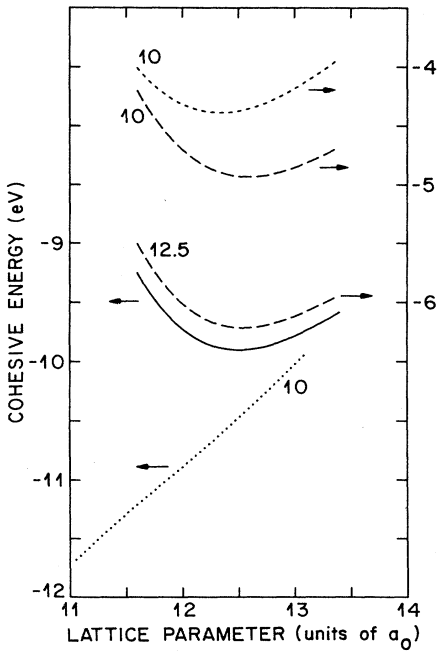

FIG. 6. Cohesive energy vs lattice parameter for LAPW calculations (solid line), Fig. 2 pseudopotentials (dotted line), Fig. 3 pseudopotentials (long-dashed line), and a separable form of the Fig. 3 pseudopotentials (short-dashed line). K^2_{max} is indicated for the pseudopotential curves.

TABLE II. Structural energy results for BaSe.

Type	K^2_{max} (Ry)	a/a_0	B (Mbar)
PW	10.0	12.59	0.415
PW	12.5	12.54	0.436
LAPW		12.51	0.450
Expt.		12.47[a]	

[a]Reference 18.

V. DISCUSSION

A generalized form of the norm-conserving pseudopotential[1,2] offers the convenience of using a single atomic reference configuration, generally the ground state. Greater flexibility is available in optimizing the properties of the pseudopotential, such as its range, strength, number of bound states, and energy of maximum accuracy. A separable form can be constructed where desired for computational efficiency.[8] Purely repulsive potentials from closed shells are possible.

Illustrative calculations of potentials for Ba and Se atoms with two choices of ionic valence show that they can be as similar to or as different from conventional bound-state NCPP's (Refs. 1 and 2) as desired for a given application. Plane-wave calculations of the band structure and energy of BaSe illustrate the performance of the GNCPP's compared with full-potential reference calculations. The poor performance of those pseudopotentials which included only the Se $4p$ and Ba $6s$ electrons outside the core for structural energies, and of the separable form for band structure, indicates the necessity of checking potentials for desired applications. Additional flexibility creates additional opportunity to make errors.

A final point which should be noted is the importance of examining plots of the pseudopotentials to make sure they "look right." The most common problem is a significant oscillation around r_{cl}, which indicates a poor choice of this parameter or placing ε_l too close to an unwanted bound state. While the effects of visible smoothness have not been systematically explored, experience has indicated that it contributes both to transferability (in the sense of performing well over a wide energy range) and convergence with basis size. Figures 2 and 3 here, as well as various figures in Refs. 1, 2, and 8, give reasonable guidance as to what the potentials should look like.

Note added in proof. Preliminary versions of this program, dated prior to June 7, 1989, contained errors and should be corrected or replaced. The factor γ_l in Eq. (12) was omitted, and the Hedin-Lundqvist exchange-correlation potential section was incorrect.

ACKNOWLEDGMENTS

The author thanks M. Foulkes, R. W. Jansen, and J. W. Davenport for helpful comments on the program for producing GNCPP's.

APPENDIX

A Fortran program has been written and tested which carries out all the steps necessary to construct GNCPP's. Copies of this program, along with input data files for all atoms (excepting lanthanides and actinides) and a sample output file, are available from the author on request (on a 5.25 in floppy disk). The structure of the program is briefly outlined below.

Basic input data consist of atomic number, number of core and valence states, and principal quantum number l and occupation of each. The Wigner,[19] Hedin-Lundqvist,[20] or Ceperly-Alder[21] form of the exchange-correlation energy may be specified. An appropriate logarithmic radial mesh and an approximate Thomas-Fermi potential are set up. The scalar-relativistic Schrödinger equation[10] is then solved for the core and valence states, and the charge density is accumulated. The output potential is calculated, and these calculations are iterated to self-consistency using the Anderson method.[22] Integrations for the Schrödinger equation, potential, etc. are carried out using the fourth-order Adams predictor-corrector formulas.[23] All the energy levels are included in the output for reference.

During the full-potential calculation, the position of the outermost maximum of the wave function with highest principal quantum number for each l is saved. These are used to calculate a set of r_{cl} following the guidelines of Ref. 2 and the discussion in Sec. III. Energies corresponding to occupied bound states are selected to construct the pseudopotentials for the corresponding l's, and that of the highest unoccupied state is selected for the others. At this point, additional optional input is sought to print wave functions, or to change the output mesh, r_{cl}'s, or unoccupied ε_l's. The screened pseudopotential is then calculated for each l in turn, following the steps in Sec. III. To test the consistency of our numerical integration of Schrödinger's equation and its analytic inversion in Eq. (12), it is solved numerically again using the final potential, either for a bound or generalized pseudo-wave-function, and the bound-state energy, and value and slope at the matching point are compared to reference values from the full-potential calculation. Discrepancies in these tests indicate a poor choice of r_{cl} or ε_l. The pseudocharge density is accumulated for the occupied states. After all the $V_{2l}(r)$ are calculated, a numerical implementation of Eq. (14) is used to unscreen them and produce $V_l^{\rm ion}(r)$.

All quantities to be output are interpolated onto a linear radial mesh using cubic splines.[24] Two sets of output are given, each including the radial mesh and the atomic pseudocharge density. The first set also includes the standard $V_l^{\rm ion}(r)$, while the second includes $rQ_l^{\rm ion}(r)$ from Eq. (18) and, as a final row, C_l from Eq. (19) for the separable form.[8]

The total energy of the valence electrons is computed to serve as a reference for cohesive energy calculations. For open-shell atoms, a local-spin-density calculation should be used to obtain a better estimate of the atomic energy. The spin-polarization correction to the atom valence energy should be obtained from a full-potential calculation because of the nonlinearity of the exchange-correlation energy. This can then be added to the pseudoatom energy calculated in this program.

[1]D. R. Hamann, M. Schlüter, and C. Chiang, Phys. Rev. Lett. **43**, 1494 (1979).
[2]G. B. Bachlet, D. R. Hamann, and M. Schlüter, Phys. Rev. B **26**, 4199 (1982).
[3]M. T. Yin and M. L. Cohen, Phys. Rev. B **26**, 5668 (1982); **26**, 3259 (1982); Phys. Rev. Lett. **45**, 1004 (1980).
[4]C. Woodward and A. B. Kunz, Phys. Rev. B **37**, 2674 (1988).
[5]S. B. Louie, S. Froyen, and M. L. Cohen, Phys. Rev. B **26**, 1738 (1982).
[6]A preliminary report of this work has been presented. D. R. Hamann, Bull. Am. Phys. Soc. **33**, 803 (1988).
[7]R. Car and M. Parrinello, Phys. Rev. Lett. **55**, 2471 (1985).
[8]L. Kleinman and D. M. Bylander, Phys. Rev. Lett. **48**, 1425 (1982).
[9]D. C. Allan and M. P. Teter, Phys. Rev. Lett. **59**, 1136 (1987).
[10]D. D. Koelling and B. N. Harmon, J. Phys. C **10**, 3107 (1977); H. Gollish and L. Fritsche, Phys. Status Solidi B **86**, 145 (1978); J. H. Wood and A. M. Boring, Phys. Rev. B **18**, 2701 (1978).
[11]L. Kleinman, Phys. Rev. B **21**, 2630 (1980).
[12]G. B. Bachelet and M. Schlüter, Phys. Rev. B **25**, 2103 (1982).
[13]F. Herman and S. Skillman, *Atomic Structure Calculations* (Prentice-Hall, New Jersey, 1963).
[14]R. W. Shaw and W. A. Harrison, Phys. Rev. **163**, 604 (1967); W. C. Topp and J. J. Hopfield, Phys. Rev. B **7**, 1295 (1974).
[15]L. Kleinman, private communication.
[16]D. R. Hamann, Phys. Rev. Lett. **42**, 662 (1979); L. F. Mattheiss and D. R. Hamann, Phys. Rev. **33**, 823 (1986).
[17]A. Baldereschi, Phys. Rev. B **7**, 5212 (1973); D. J. Chadi and M. L. Cohen, *ibid.* **8**, 5747 (1973); H. J. Monkhorst and J. D. Pack, *ibid.* **13**, 5188 (1976).
[18]R. W. G. Wyckoff, *Crystal Structures*, 2nd ed. (Krieger, Malabar, Florida, 1982), Vol. 1, p. 86.
[19]E. Wigner, Phys. Rev. **46**, 1002 (1934).
[20]L. Hedin and B. I. Lundqvist, J. Phys. C **4**, 2064 (1971).
[21]D. M. Ceperley, Phys. Rev. B **18**, 3126 (1978); D. M. Ceperley and B. J. Alder, Phys. Rev. Lett. **45**, 566 (1980); J. Perdew and A. Zunger, Phys. Rev. B **23**, 5048 (1981).
[22]D. R. Anderson, J. Assoc. Comput. Mach. **12**, 547 (1965).
[23]P. J. Davis and I. Polonsky, in *Handbook of Mathematical Functions*, edited by M. Abramowitz and I. A. Stegun (Dover, New York, 1965), p. 896.
[24]W. H. Press, B. P. Flannery, S. A. Teukolsky, and W. T. Vetterling, *Numerical Recipes* (Cambridge University Press, Cambridge, 1986), pp. 86–89.